



# Influence of annealing on the morphology and mechanical properties of iPP/HDPE blend with tailored oriented crystalline structures

Xuanbo Gu<sup>1</sup> · Man Zhou<sup>1</sup> · Yingxiong Wang<sup>1</sup> · Jie Zhang<sup>1</sup>

Received: 21 February 2019 / Accepted: 15 July 2019 / Published online: 24 July 2019  
© The Polymer Society, Taipei 2019

## Abstract

In this article, two kinds of isotactic polypropylene (iPP)/high density molecular weight polyethylene (HDPE) blend samples were prepared by an accessible injection-molding method. These two samples contain iPP shish kebab matrix and HDPE dispersed phase (shish kebab and epitaxy crystal, respectively). The variation of microstructures upon annealing was characterized using scanning electron microscopy, differential scanning calorimetry and small-angle X-ray scattering. It was found that the variations of different crystalline structures were changed by varying annealing parameters. Only the rearrangement of partially melted chains into primary lamellae happened for the sample with epitaxy crystalline structure, which was distinguished from the sample with HDPE shish kebab structure. Moreover, the variation of the crystalline structure, crystallinity and melting point were discussed to account for the changes in mechanical properties. These results revealed the relationship among the morphology, annealing parameters and mechanical properties, which provide a practical method to industrial manufacture.

**Keywords** Annealing · Epitaxy crystalline · Shish-kebab · Mechanical properties · Blend

## Introduction

Heat treatment can improve polymer's properties by removing the residual stress in polymer products, perfecting the crystalline structure and vanishing the crystal defects which are usually generated during the processing such as injection molding and extrusion [1–5]. As a result, annealing is a useful post-processing technology to adjust the microstructure of polymers [6–11]. For semi-crystalline polymers, annealing will not only affect the arrangement of polymer chains in amorphous region, but also the structure of crystalline region. It is determined by the specific parameters of annealing. A temperature between the glass transition temperature  $T_g$  and the melting temperature  $T_m$  is chosen as the annealing temperature due to the improved chain mobility in amorphous region and the partially changed structure in the crystalline area under this condition, which are beneficial to the perfection of crystallization [12]. Usually, the annealing time depends on the

temperature. Although longer annealing time can result in better crystallization [7, 9, 12], the effect is limited. That is, increasing annealing temperature is more effective than prolonging annealing time with the aim to adjust the crystalline structure.

Importantly, different crystalline structures have different variations during annealing process. For isotactic polypropylene (iPP) spherulites, their number will not be changed by annealing while the mobility of polymer chains will be improved and thus some chains can move into crystalline region, increasing the lamellae thickness and crystallinity [5, 12, 13]. Compared to the isotactic structure, the highly oriented crystalline structures have characteristic variations during annealing. For example, the shish kebab of iPP composing highly oriented shish and kebab lamellae growing on it has more complicated variations upon annealing than spherulites. As far as we know, the melting temperature of shish is higher than the kebab. That is, the thermal stability of shish is much better [14, 15]. Besides the perfecting phenomenon of the kebab lamellae just like spherulites, new kebab lamellae composing relaxed molecular chains in the amorphous phase could be induced by the shish because there are still nucleating sites on it [6, 9]. What's more, some researches reveal that during annealing the lamellae sliding and dispersing can thicken the lamellae and therefore extend the long period [5, 13]. As a

✉ Jie Zhang  
zhangjie@scu.edu.cn

<sup>1</sup> College of Polymer Science and Engineering, State Key Laboratory of Polymer Materials Engineering, Sichuan University, Chengdu 610065, China

matter of fact, the shish kebab structure was regarded as a polymer self-reinforced structure which can bring improved mechanical strength, toughness [16, 17] and creep behavior [18]. And the mechanical properties of shish kebab can also be enhanced upon annealing because of the perfection of microstructure [2, 6, 19].

As another highly oriented crystalline structure, epitaxy crystalline has attracted intensive research interests. For PP/PE blends, the geometric lattice matching for (100) lattice plane of PE and (010) lattice plane of iPP is responsible for the special inclined lamellae arrangement [20–22]. This special inclined arrangement can provide excellent mechanical properties [20, 23], especially impact strength [24] by enhancing the interfacial adhesion of two phases which facilitates the transmission and dissipation of external force. Gross [20] firstly obtained epitaxy crystalline structure in PP/PE film and tested its mechanical properties. To obtain this structure, his method contained two steps: (1) Fabrication of PP/PE multi-layer film by using melt drawing method, (2) Melting and recrystallization of PE on oriented PP phase by heat treatment. The results showed that both the Young's modulus and fracture stress of annealed sample were improved, which could be explained that the enhanced interfacial adhesion resulted from the insert of PE lamellae into PP crystalline structure. However, this conventional method is time-taking and effort-consuming. With the development of practical processing technology in decades, Fu's research group [25–27] obtained this structure by using dynamic packing injection molding, indicating that extensive shear field was beneficial to the formation of epitaxy crystalline structure. But the structure obtained in their samples was only in the shear layer, which occupied less than the half of the sample on thickness direction. Therefore, the mechanical tests always involved other regions without epitaxy structure, which should be avoided to carefully investigate the relationship between morphology and mechanical properties. Hence, the influence of annealing on the morphology and mechanical properties of epitaxy crystalline structure is still mysterious due to the technological limitation on preparing the sample with pure epitaxy structure.

Recently, our research group developed a new technology named multi-flow vibration injection molding (MFVIM) [28, 29] which could bring strong shear effect within the whole sample even in the core region. The specific process of MFVIM are as following: after the mold is fully filled, the vibration pressure can be introduced into mold cavity during packing stage. Simultaneously, a part of existed melt will be pushed out of the mold cavity and the shear field occurs with the aid of a designed flash groove. Therefore, samples with fully oriented structures can be prepared, which is very different from the conventional injection molded ones with typical "skin-core" structure. Deng made a conclusion in his search [30] that the mold temperature played an important role on epitaxy crystallization. It suggested that a higher mold

temperature between the melting points of iPP and HDPE was beneficial for the relaxation of molecular chains, making PE chains crystallize onto PP oriented crystalline. These results make it possible to fabricate epitaxy crystalline structure occupying the whole sample without post-processing step.

In this paper, we directly obtained two kinds of iPP/HDPE samples with highly oriented crystalline structures by using a self-designed multi-flow vibration injection molding (MFVIM) device with different mold temperatures. The blend samples compose of iPP oriented matrix (shish kebab) occupying almost the whole sample and HDPE dispersed oriented structure (shish kebab in sample A and epitaxy crystalline structure in sample B, respectively). Then, these two kinds of samples were annealed at several temperatures between  $T_g$  and  $T_m$  to adjust the crystalline morphology and optimize the mechanical properties. Polarized light microscopy (PLM) and scanning electron microscopy (SEM) were used to get direct information about the morphology, the crystallinity and melting points were characterized by differential scanning calorimetry (DSC). And by using the small-angle X-ray scattering (SAXS), the variation of the crystalline structure upon annealing can be certainly known.

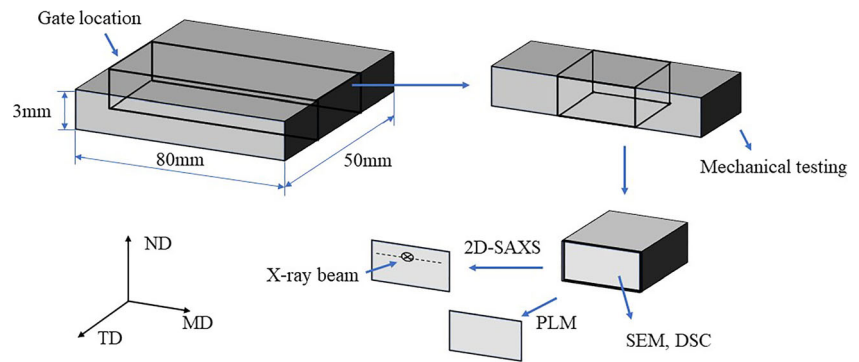
## Experimental section

### Materials and sample preparation

Isotactic polypropylene (iPP, trademark of T30S) synthesized by Ziegler-Natta catalyst, was purchased from Dushanzi Petroleum Chemical Co., China. It has a  $M_w$  of  $3.99 \times 10^5$  g/mol,  $M_w/M_n \sim 4.85$ , a melt flow rate (MFR) of 2.90 g/10 min (230 °C, 2.16 kg), a density of 0.91 g/cm<sup>3</sup> and a tacticity of 96.0%. High density polyethylene (HDPE, trade name 5000S) was purchased from Lanzhou Petroleum Chemical Co., China. It has a  $M_w$  of  $3.73 \times 10^5$  g/mol,  $M_w/M_n \sim 4.3$ , a melt flow rate (MFR) of 1.18 g/10 min (190 °C, 2.16 kg), a density of 0.95 g/cm<sup>3</sup>.

First, HDPE and iPP were melted together by a SHJ-25 corotating twin-screw extruder with a weight ratio of 20/80. The screw speed was 120 rpm and the temperature profile were 150–200 °C from hopper to nozzle. Then, the dried pellets were injection molded by MFVIM to prepare iPP/HDPE samples (80mm × 50mm × 3mm, as shown in Fig. 1) with almost fully oriented structures. The mold temperature was set as 40 °C (sample A) and 135 °C (sample B) respectively to get two kinds of samples. For sample B, the mold temperature was turned down after the packing stage finished to enable the part to cool down. The preparation method and theory details were described previously [24]. The annealing temperatures were chosen as 105, 125 and 145 °C, and the annealing time were chosen as 2 h and 6 h.

**Fig. 1** The schematic drawing of sampling methods. MD: melt flow direction, TD: transverse direction, ND: normal direction



## Polarized light microscopy

Thin slices were cut by microtome for optical morphology observations. One middle position of the sample was used to represent the whole part because the whole sample shows almost the same structure. PLM observations were performed by using a DX-1 (Jiang Xi Phoenix Optical Co., China.) microscope connected with a Nikon 500D digital camera.

## Scanning Electron microscopy

A solution of 8:4:1 volume of concentrated sulfuric acid, phosphoric acid and distilled water was prepared (1.5 g of potassium permanganate in 100 mL of mixture) [31]. The samples were cut along the flow direction (as shown in Fig. 1) and then immersed in the solution at 60 °C for 7 h to dissolve away the amorphous phase. After it, the samples were covered with a thin layer of gold by sputtering and observed by a field emission SEM (Inspect-F, Fei, Finland) with an acceleration voltage of 15 kV to observe the crystalline morphology of the blends.

## Two-dimensional small-angle X-ray scattering

Two-dimensional small-angle X-ray scattering (2D-SAXS) measurements were carried out in the Shanghai Synchrotron Radiation Facility (SSRF). The wavelength of the X-ray was 0.124 nm and the rectangular beam had dimensions of 0.5 mm × 2 mm. A MAR CCD X-ray detector (MARUSA) was employed to detect 2D-SAXS images. The distance between sample and detector was 1910 mm. The sample was mounted on a three-dimensional elevator platform with its thickness direction parallel to the Y-axis. One position (700 μm down from surface) was scanned (shown in Fig. 1).

## Differential scanning calorimetry (DSC)

The analysis of the thermal behavior of crystallization and the crystallinity of each component was carried on a TA-Q200 differential scanning calorimetry instrument under a nitrogen atmosphere. Specimens (Fig. 1) about 5 mg were placed in a

sealed aluminum pan and then were heated to 200 °C at a heating rate of 10 °C/min. The crystallinity  $X_c$  of component  $i$  was calculated accordingly by the following equation:

$$X_c = \frac{\Delta H_i}{\Delta H_i^m \varphi_i}$$

Where  $\Delta H_i$  obtained from DSC directly is the enthalpy of fusion of component  $i$ , and  $\Delta H_i^m$  corresponding to the enthalpy of fusion of 100% crystalline polymer is 293 and 207 J/g for HDPE and iPP, respectively [27]. The value  $\varphi_i$  is the mass fraction of component  $i$  in the blend.

## Mechanical properties

The measurements of mechanical properties were carried on at room temperature. A RGT-10 computer controlled electronic universal testing machine was used to measure the tensile properties of dumbbell-shape specimens at a crosshead speed of 50 mm/min according to ASTM D-638. And the Izod notched impact strength was measured using a UJ-40 Izod machine according to ASTM D256–04. The values were calculated as averages of over five samples for each composition.

## Results and discussion

### Crystalline morphology

As shown in Fig. 2(a) and (b), the samples were observed by PLM firstly which can reflect the morphologies about the whole samples. The colorful areas pointed out by the yellow arrows and lines refer to the highly oriented crystalline structure occupying almost the whole range of samples, while the dark regions in the center corresponding to the typical isotropy structure has a narrow width which can almost be ignored. It demonstrates that the samples with fully oriented structures were successfully prepared by using MFVIM technology. Although different mold temperatures were chosen to form two kinds of highly oriented crystalline structures, similar thickness of shear layers can be obtained by adjusting the

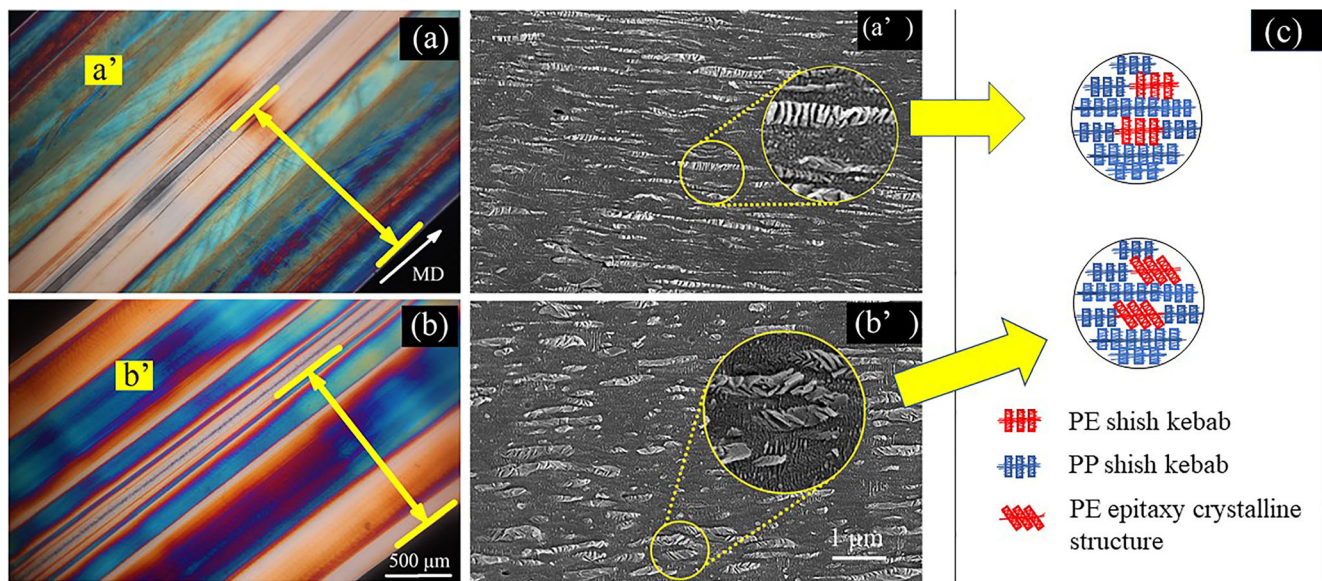


**Fig. 2** PLM pictures of sample **a** (a) and sample **b** (b), corresponding SEM micrographs (a'), (b') of the marked areas with enlarged pictures, and their schematic diagrams (c). The flow direction is horizontal in SEM micrographs

processing parameters. However, due to the resolution limitation of the PLM pictures, further characterizations are needed for detailed differences of these two samples.

Figure 2(a') and (b') shows the SEM micrographs down from the surface about 700  $\mu\text{m}$  of samples, in which the relatively dark region refers to the PP phase and white area PE phase considering different resistance ability to etching solution and their weight ratio (80:20). Therefore, it is easy to recognize that the PP phase shows as the matrix while the PE phase well disperse in it. In Fig. 2(a'), it can be seen clearly that the kebab lamellae are all arranged perpendicular to the flow direction, which means PP and PE phases both form their own shish kebab structures in the blend. However, when the mold temperature is higher (135  $^{\circ}\text{C}$ ), although the PP phase is still shish kebab the PE phase exists as particular inclined crystalline lamellae, i.e., epitaxy crystalline structure, as shown in Fig. 2(b').

The formation of these two kinds of special crystalline structures are resulted from the MFVIM by setting relevant parameters. Different from conventional injection molding which provides only one melt flow causing a typical skin/core structure, the MFVIM technology can provide several extra melt flows with settled interval time during packing stage. Thanks to this special process, samples with a thickened "skin" and a narrowed "core" can be prepared. For the lower mold temperature, the shish kebab of semi-crystalline polymer caused by shear field can be kept. However, things change dramatically when the mold temperature was settled at 135  $^{\circ}\text{C}$  which is higher than PE melting point but lower than that of PP. In sample B the PP phase still formed its shish kebab structure as sample A, while the PE phase suffered the same shear flow field which made the extension of PE

chains along the injection molding direction and then relaxed to form epitaxy structure. This is fundamentally because that PP and PE have lattice matching relationship between (010) lattice plane of PP and (100) lattice plane of PE. Therefore, PE phase was supposed to crystallize into epitaxy crystalline structure when PP formed shish-kebab structure as the matrix. According to the research [24, 32, 33], the orientation of PP matrix and proper cooling rate were both important parameters, which can determine the final morphology of PE. Thus, it can be regarded that the intensive shear flow field and proper recrystallization process is necessary for the formation of epitaxy structure. Finally, the mold temperature was turned down to a lower one (40  $^{\circ}\text{C}$ ) for the sample cooling when the injection and packing processes finished.

### Influence of annealing on crystalline morphology

Figure 3 shows the crystal morphology of sample A after annealing at different temperatures and times. As discussed above, in sample A both PP phase and PE phase exist as shish kebab structure, as shown in Fig. 2. It can be seen there is almost no change of the crystalline structure between unannealed sample (Fig. 2(a')) and the sample after annealing at the temperature of 105  $^{\circ}\text{C}$  (Fig. 3A<sub>1</sub>), even prolonging the time from 2 h to 6 h (Fig. 3A<sub>4</sub>). It is because this temperature is far below the melting temperature (about 130  $^{\circ}\text{C}$ ) of PE and cannot affect the crystalline structures obviously. By raising the temperature to 125  $^{\circ}\text{C}$ , the structure of crystalline has no significant difference but the arrangement of the lamellae becomes more compact, especially for PE phase (Fig. 3A<sub>2</sub>). It illustrates that partial melting and re-crystallization happens in amorphous phase because 125  $^{\circ}\text{C}$  is close to PE melting

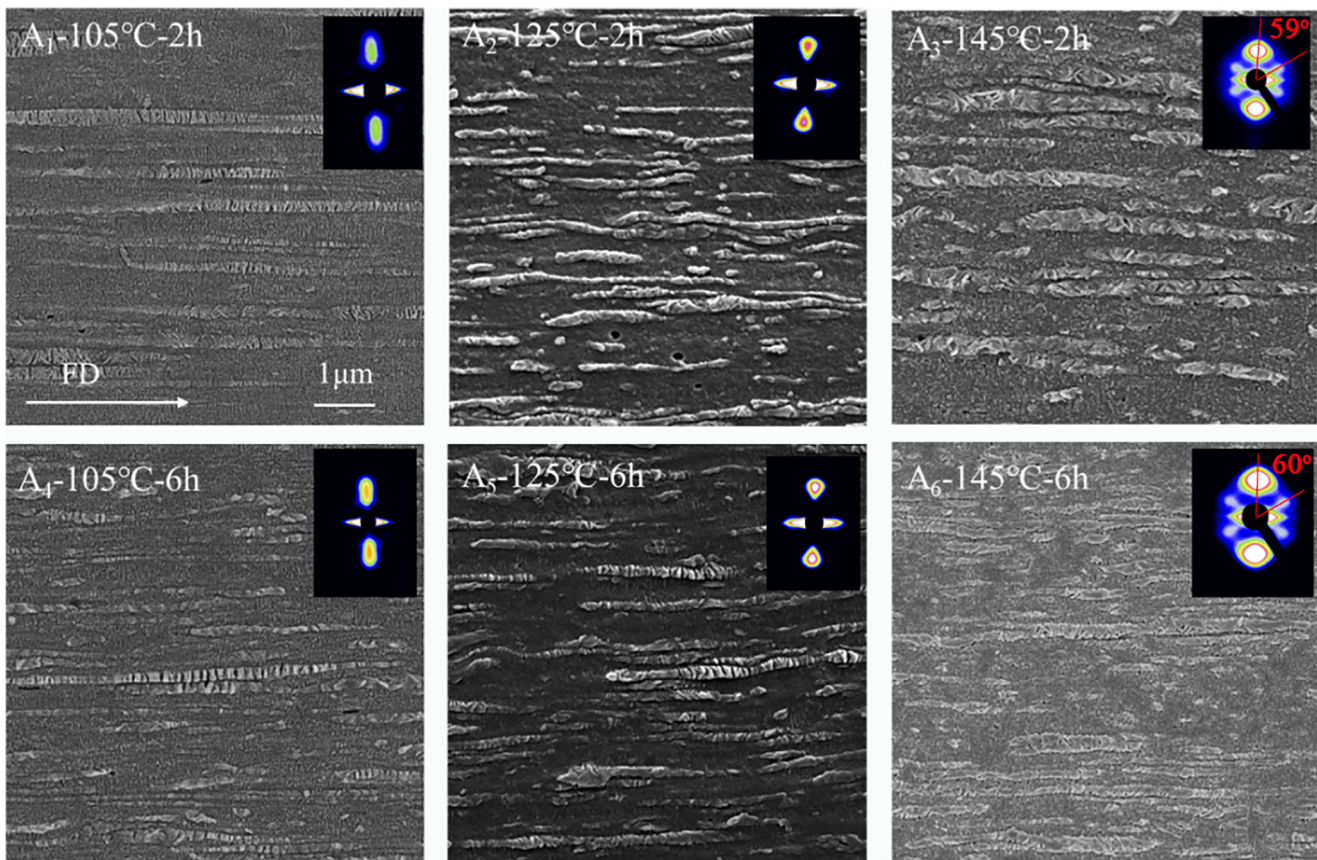


**Fig. 3** SEM micrographs and corresponding 2D-SAXS patterns of sample A. The flow direction is horizontal for SEM but vertical for SAXS

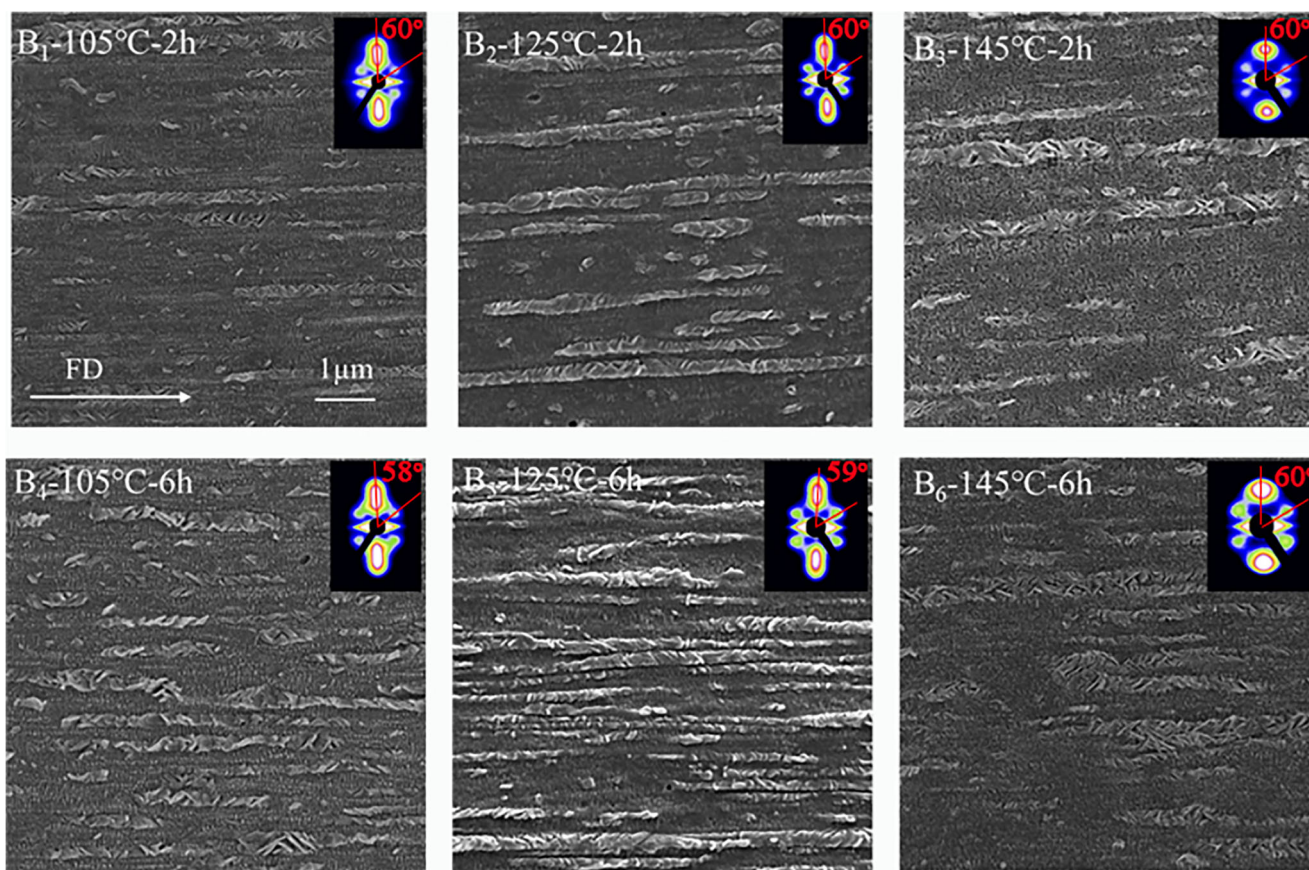
temperature. And this phenomenon becomes more obvious with the longer time (Fig. 3A<sub>5</sub>). It can also be found in the 2D-SAXS patterns that at 125 °C the signal of kebab is stronger (Fig. 3A<sub>2</sub> and A<sub>5</sub>). Things have a significant change at 145 °C, the PP is still shish-kebab, whereas the PE epitaxy crystalline structure is formed, which can be confirmed by the 2D-SAXS patterns (Fig. 3A<sub>3</sub> and A<sub>6</sub>). And it can be confirmed from the patterns that the average epitaxial growth angles are around 60°, all larger than classical epitaxy theory value of 50°. It can be ascribed to the differences between MFVIM and classical epitaxy theory, and the intensive melt flow field should be responsible for it [34]. Moreover, it demonstrates that when the annealing temperature is between the melting temperatures of PE and PP, the oriented chains of PE would like to melt and re-crystallize, but the shish kebab of PP could be kept. Thus, the relaxed PE chains epitaxially grow onto oriented PP lamellae and finally form the inclined lamellae structure like that in sample B. Furthermore, there is no significant change by prolonging the annealing time, which demonstrates that 2 h is enough to induce melting and re-crystallization. The change of crystalline structure including lamellae thickness will be discussed later with other experiment results.

Figure 4 shows the crystalline morphology of sample B after annealing. In sample B, the structure of PP is shish kebab, and the PE phase exists as epitaxy structure. All the

samples have the average inclined angles of about 60°. And there is no other significant morphology change, no matter raising the temperature or prolonging the time. However, it should be noted that the epitaxy crystalline is newly formed by melting and re-crystallization of initial epitaxy crystalline structure considering the variation in the sample A when the annealing temperature is 145 °C. Detailed crystalline structure variations will be discussed in lateral parts with the 2D-SAXS patterns.

### Influence of annealing on crystalline melting behavior

The crystallinity and melting point of PP and PE in the blend measured by DSC are listed in Table 1 and Table 2, respectively. Considering that annealing can perfect crystalline structure, the crystallinity of PE phase expectedly improves with the increase of annealing temperature. But when the temperature is the same, the crystallinity only has a slight variation by prolonging the annealing time from 2 h to 6 h. It shows that around PE melting temperature, the perfection of PE crystalline structure could be finished within 2 h. And as for the PP phase, the crystallinity has a significant improvement only when the annealing temperature is 145 °C. That is, the relatively lower temperatures will not affect the structure of the



**Fig. 4** SEM micrographs and corresponding 2D-SAXS patterns of sample B. The flow direction is horizontal for SEM but vertical for SAXS

crystalline region and amorphous phase obviously because the melting temperature of PP is 165 °C. It can be concluded that partial recrystallization in the amorphous region happened when the temperature is 145 °C. Moreover, the influence of annealing time on PP phase is determined by the temperature. Prolonging annealing time has no effect on the crystallinity at the lowest temperature (105 °C), but it works at 125 °C and 145 °C for PP phase due to the improvement of chain mobility under the temperatures which are beneficial for crystallization. Compared to crystallinity, the melting points have a slighter change whose trend is similar in that of crystallinity. It is worth noting that the melting point of PP has a relatively obvious improvement when the annealing temperature is 145 °C for

6 h, which corresponds to the significant change in crystalline structure, such as the relaxation of chains, partially melting in amorphous phase and the thickening of lamellae in the crystalline region.

### Influence of annealing on lamellae structure

Considering the above results, a quantitative study of lamellae structure was carried out by following equations [35–37].

$$L = 2\pi/q \quad (1)$$

$$L_c = L \times X_c \quad (2)$$

**Table 1** Crystallinity of different components of annealing samples

Sample		A			B		
		105 °C	125 °C	145 °C	105 °C	125 °C	145 °C
PE phase	unannealed	0.454			0.499		
	2 h	0.501	0.523	0.586	0.520	0.558	0.613
	6 h	0.499	0.513	0.564	0.533	0.583	0.575
PP phase	unannealed	0.331			0.341		
	2 h	0.355	0.349	0.440	0.352	0.357	0.453
	6 h	0.358	0.375	0.482	0.362	0.406	0.504

**Table 2** Melting point of different components of annealing samples

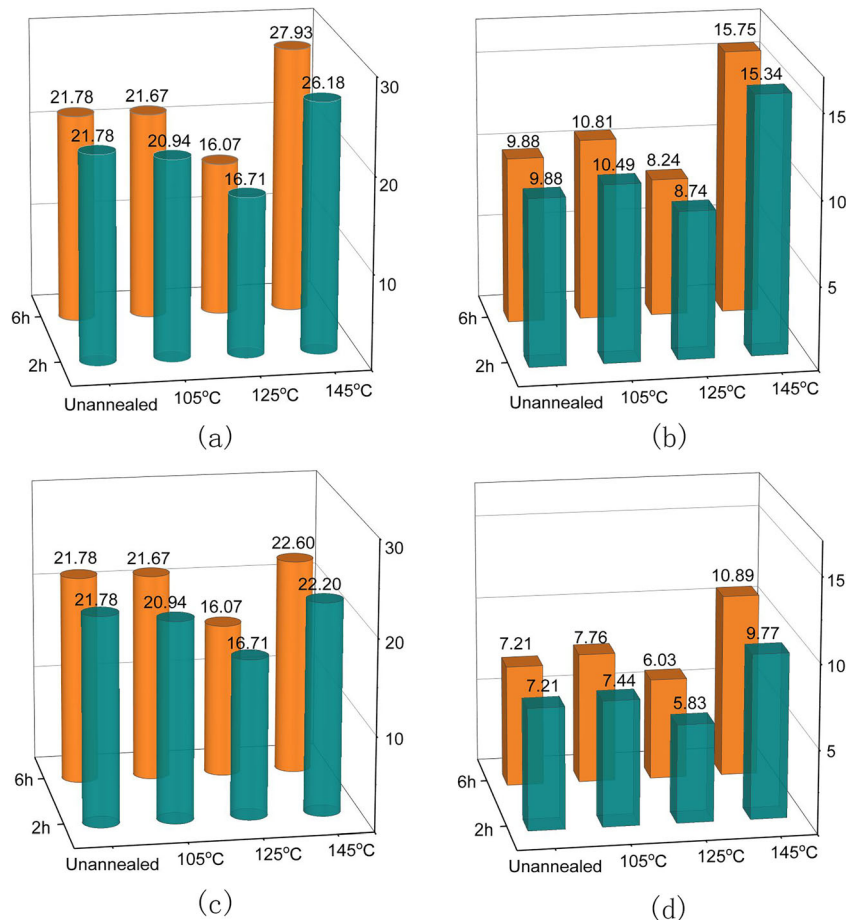
Sample		A			B		
		105 °C	125 °C	145 °C	105 °C	125 °C	145 °C
PE phase	unannealed	128.4			129.2		
	2 h	129.2	129.8	131.4	129.1	132.0	131.0
	6 h	129.4	130.2	131.3	130.0	130.3	130.6
PP phase	unannealed	164.4			165.6		
	2 h	165.0	165.0	166.3	165.2	165.3	166.9
	6 h	164.7	165.9	169.2	165.1	165.9	167.9

$$L_a = L - L_c \tag{3}$$

The eq. (1), Bragg diffraction equation, was used to calculate the long period  $L$ , in which  $q$  is the corresponding horizontal value of the peak in the scattering curve. Eq. (2) was used to calculate the lamellar thickness  $L_c$ , where  $X_c$  is the crystallinity from DSC. And the thickness of amorphous phase  $L_a$ , was calculated by eq. (3) because the long period concludes both crystalline region and amorphous phase.

It should be noted that for sample A, the signals of PP and PE overlap with each other because of the same structure of shish kebab. Thus, the calculated long period is regarded as an average value for the two phases. While the kebabs can be distinguished from 2D-SAXS for sample B, which came from different kebab structures (the kebab perpendicular to the flow direction and the inclined one). In view of the above discussion, we only analyzed long period and lamellar thickness of sample A (Fig. 5), but long period, lamellar thickness and the thickness of

**Fig. 5** Variation of long period (nm) for different components of sample A after annealing: (a) PE phase, (c) PP phase. And the thickness of lamellae (nm): (b) PE phase, (d) PP phase



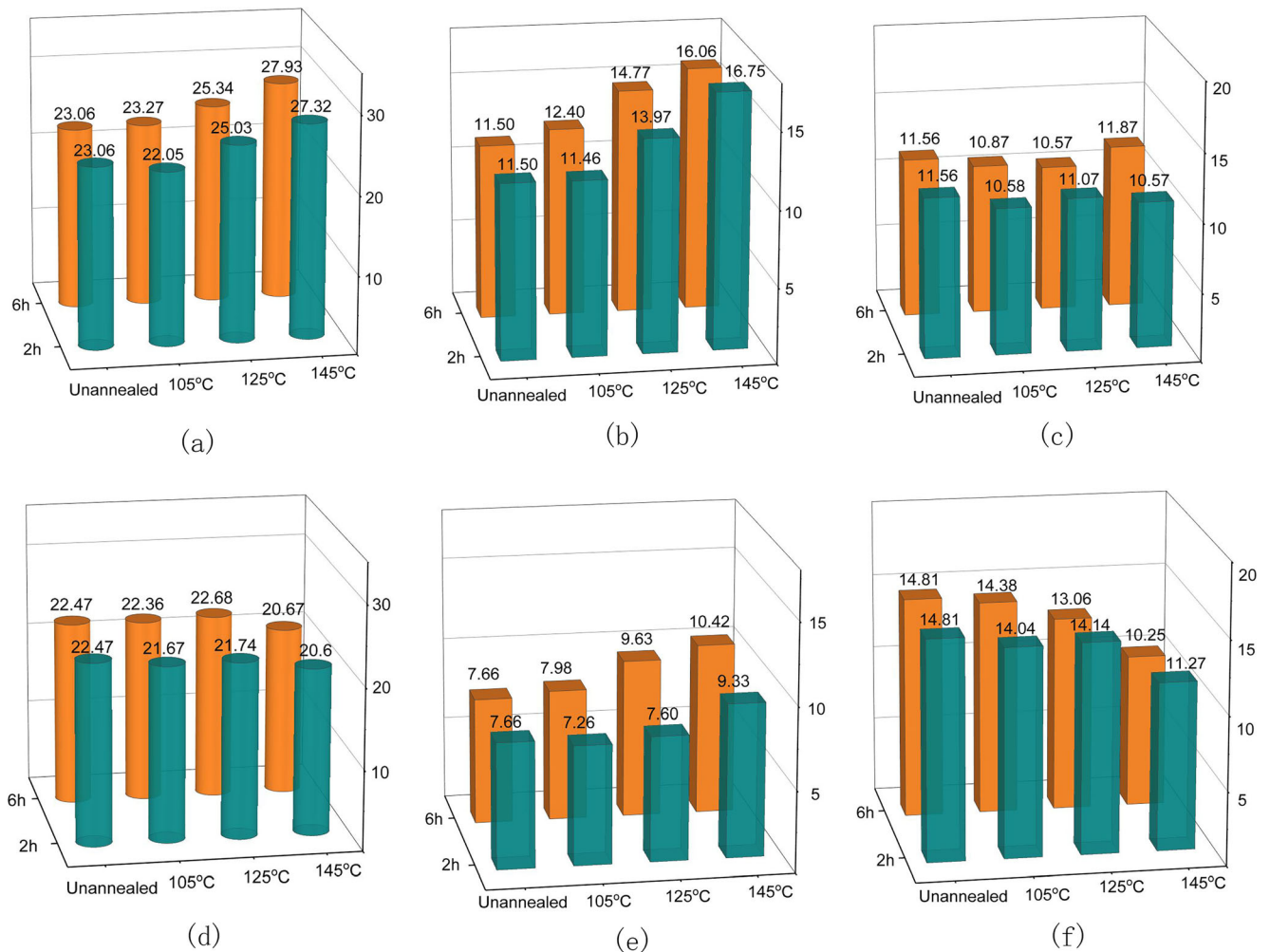
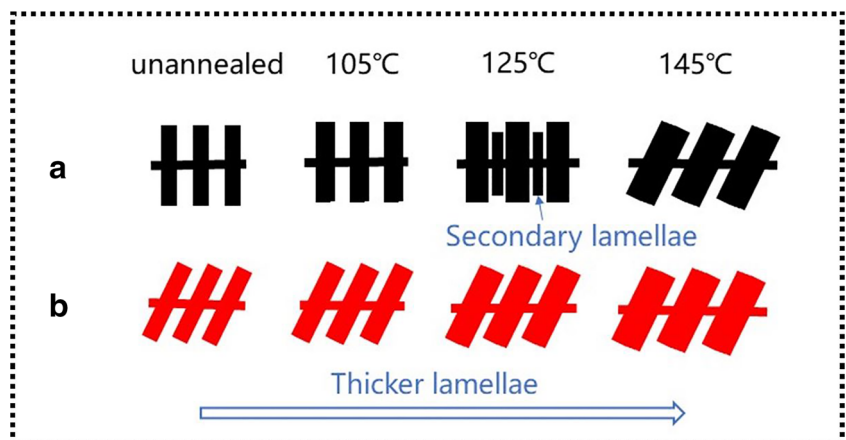


**Fig. 6** Variation of long period (nm) for different components of sample B after annealing: **(a)** PE phase, **(d)** PP phase. And lamellar thickness (nm): **(b)** PE phase, **(e)** PP phase. And the thickness of amorphous region (nm): **(c)** PE phase, **(f)** PP phase

amorphous phase for sample B (Fig. 6). And a schematic variation of PE phase in sample A and B at different annealing temperatures is shown in Fig. 7 to better understanding the difference between shish kebab structure and epitaxy crystalline structure after annealing.

For sample A, the average long period and lamellar thickness of PP and PE phases have no significant change after annealing at 105 °C, illustrating that this annealing temperature is not high enough to change the microstructure obviously. Whereas the average long period and lamellar thickness

**Fig. 7** A schematic variation of PE phase of sample A and B after annealing at different temperatures





both decrease with the increase of annealing temperature from 105 °C to 125 °C, which should be ascribed to the change of PE phase. Because annealing at 105 °C or 125 °C has a slight influence on PP phase whose melting point is around 165 °C and the beginning temperature of melting is about 135 °C. The DSC results (as shown in Table 1 and Table 2) also demonstrate that both the melting point and the crystallinity have no obvious variation for PP phase. Thus, the average method for calculating long period can be used to discuss the variation of PE phase. As a result, we speculated two possible reasons for change of PE phase: the melting and recrystallization of imperfect crystalline; the second crystallization and the transition from smectic phase to crystalline phase in amorphous. Each reason will induce the generation of secondary lamellae rather than simply lamellae thickening, as shown in Fig. 7. Hence, the sample has a higher crystallinity, a stable melting point and a decreased long period and lamellar thickness with the temperature raising from 105 °C to 125 °C.

As the temperature reaching 145 °C, the long period and lamellar thickness are both increased compared to those at 125 °C. It is worth noting that the PP is shish kebab structure while the PE is epitaxy structure because PE phase containing primary and secondary kebab lamellae suffers a melt and re-crystallization process at this annealing temperature. That is, the structure has a significant change, of which the long period can be calculated directly from SAXS pattern rather than using the average method. It can be confirmed that the long period and lamellar thickness of PE both have remarkable improvement when it re-crystallizes into epitaxy structure. However, the annealing time has a tiny influence on the crystalline structure because prolonging the annealing time can only increase the long period and lamellar thickness with limited values, which demonstrates that the transition of the crystalline structure during annealing has almost completed within 2 h.

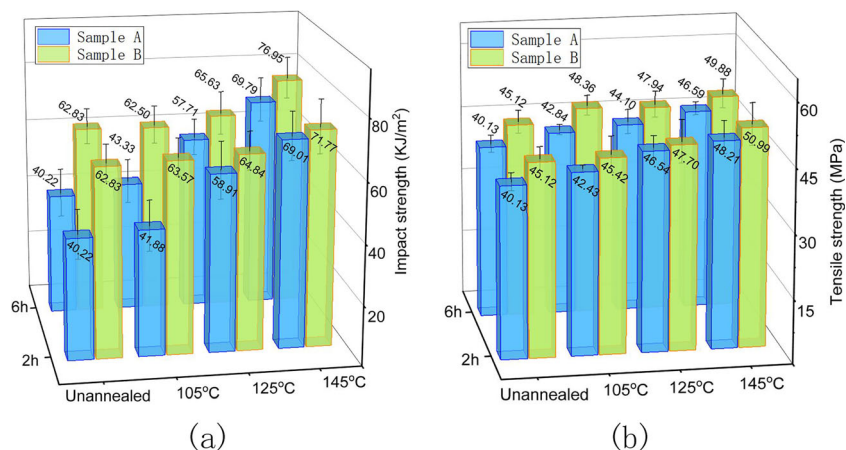
The variation of sample B during annealing is more complicated than that of sample A. The analysis was carried out on long period, lamellar thickness and the thickness of amorphous phase as shown in Fig. 6. For PE phase, with the improvement of temperature to 145 °C both long period and lamellar thickness increase gradually but the thickness of amorphous phase changes slightly, which demonstrates that a higher annealing temperature can perfect the PE epitaxy structure and thicken the lamellae that is different from PE shish kebab. The reasons are as follows: the amorphous phase of PE would partial melt and the chains get rid of the “frozen” state at 125 °C. Then, these chains tend to form newly secondary lamellae on the original shish by recrystallization for the shish kebab structure. While for the epitaxy structure, because the lamellae structure of PE epitaxially grows on the oriented PP lamellae with an inclined arrangement, the chains are difficult to form new lamellae but trend to arrange into the surrounding existed ones and thicken them. However, for PP

phase, the variation of crystalline structure is different at varying temperatures. The long period, lamellae thickness and the thickness of amorphous phase have no significant changes when the annealing temperature is below 145 °C. This is because the temperature is still too low to affect the crystalline structure of PP phase. Only by prolonging the annealing time to 6 h can thicken the lamellae corresponding to the improvement of the crystallinity (Table 2). When the temperature is raised to 145 °C, the increased lamellar thickness, the decreased thickness of amorphous phase and the shortened long period illustrate that after the melting of partial amorphous phase, the chains not only rearrange into the crystalline region thickening the lamellae but also form secondary lamellae on its shish (just like that of PE shish kebab at 125 °C). These phenomena also correspond to the greatly improved crystallinity from DSC results. Importantly, the variation of PP phase at 145 °C has a direct effect on the PE phase owing to the epitaxial relationship in sample B. Considering the melting and recrystallization behavior for PE phase occurs at this temperature, the lamellae thickening and the generation of secondary lamellae of PP phase give an advantage to the epitaxial re-crystallization. Therefore, the newly formed epitaxial lamellae have a longer long period and thicker lamellae compared with the original structure, as shown in Fig. 7.

## Mechanical properties

The mechanical properties are shown in Fig. 8. As far as we know, the epitaxy crystalline structure can enable much better impact strength by providing various transmission paths for the dissipation of external force rather than directly transmitting it across the material. Thus, sample B (the one with epitaxial structure) exhibits better mechanical properties, especially impact strength, which is in line with the results reported in our previous work [24]. Therefore, the variation of mechanical properties after annealing is mainly discussed in this part. The variation of impact strength (Fig. 8 (a)) has obvious trend with various temperatures. For sample A, it can be inferred that the better property of shish kebab (at 105 °C and 125 °C) mainly comes from the perfection of PE crystalline and the generation of secondary lamellae because these temperatures have tiny influence on PP phase. When the shish kebab transforms into epitaxy crystalline structure at the annealing temperature of 145 °C, the impact strength has a further enhancement from 58.91 KJ/m<sup>2</sup> to 69.01 KJ/m<sup>2</sup> (2 h' annealing treatment), demonstrating that the epitaxy structure plays an important role on the enhancement of impact strength. And for sample B, by rising the temperature to 105 °C and 125 °C, the property has a slight improvement by respective 0.74 KJ/m<sup>2</sup> and 2.01 KJ/m<sup>2</sup>, which is possibly caused by the thicker lamellae of PE phase within the stable structure of PP matrix. However, the impact strength has a great enhancement by 8.94 KJ/m<sup>2</sup> when annealing temperature is 145 °C. It can be

**Fig. 8** Mechanical properties of samples: **(a)** Izod notched impact strength and **(b)** tensile strength



inferred that the enhancement mainly comes from the further perfection of crystalline region of PP matrix which can simultaneously facilitate the formation of thickened lamellae and longer long period of the recrystallized PE phase as a synergistic effect.

For tensile strength, with the improvement of annealing temperature, there is an enhancement for both sample A and B, as shown in Fig. 8(b), which should be contributed to the perfection of the crystalline structures of the two phases at higher annealing temperatures. Although the enhancement of the tensile strength can be ascribed to epitaxy structure which can improve the interfacial adhesion of the two phases, the perfection of PP matrix plays a dominant role as the crystallinity of PP increased (shown in Table 1). Therefore, the further improvement of tensile strength by annealing is mainly due to the higher crystallinity of PP and PE phases. As annealing temperature is 145 °C, sample A and sample B have the similar structure resulting in the close property. Furthermore, the variation of annealing time has a slight influence on mechanical properties which could be ascribed to the slightly varied crystallinity of PP and PE phases.

## Conclusion

In this work, two kinds of iPP/HDPE blend samples with tailored oriented structures, namely PE epitaxy crystalline structure and PE shish kebab structure dispersed in PP shish kebab matrix within the whole sample, were successfully prepared by using the MFVIM technique. After subsequent annealing at proper temperatures, the melted chains in amorphous region of the sample with PE shish kebab structure would like to thicken primary lamellae and generate secondary lamellae. However, for the sample with PE epitaxy crystalline structure, the chains only rearrange into primary lamellae and thicken it. The inclined arrangement which could bring greater space steric hindrance may be responsible for the differences. Simultaneously, the thicker primary lamellae and the

secondary lamellae of PP phase can facilitate the thickening of lamellae and increase of long period of PE epitaxy recrystallized phase. The enhancement of impact strength and tensile strength can be respectively contributed to the improvement of the epitaxy structure and the crystallinity of materials. Additionally, the PE shish kebab would turn into epitaxy crystalline structure by annealing at 145 °C, resulting in similar properties of these two kinds of samples.

**Acknowledgements** This work was financially supported by The National Natural Science Foundation of China (No. 0030905401227). The authors also express sincere thanks to the Shanghai Synchrotron Radiation Facility (SSRF), China.

## References

- Blom HP, Teh JW, Bremner T, Rudin A (1998) Isothermal and non-isothermal crystallization of PP: effect of annealing and of the addition of HDPE. *Polymer* 39(17):4011–4022
- Ferrer-Balas D, Maspoch ML, Martinez AB, Santana OO (2001) Influence of annealing on the microstructural, tensile and fracture properties of polypropylene films. *Polymer* 42(4):1697–1705
- Frontini PM, Fave A (1995) The effect of annealing temperature on the fracture performance of isotactic polypropylene. *J Mater Sci* 30(9):2446–2454
- Pralay Maiti; Masamichi Hikosaka, ‡; Koji Yamada; Akihiko Toda, A.; Gu†, F., Lamellar Thickening in Isotactic Polypropylene with High Tacticity Crystallized at High Temperature. *Macromolecules* 2000, 33 (33), 9069–9075
- Rastogi S, Spoelstra AB (1999) Chain mobility in polymer systems : on the borderline between solid and melt 1. Lamellar doubling during annealing of polyethylene. *Macromolecules* 30(25):7880–7889
- Bai H, Deng H, Zhang Q, Wang K, Fu Q, Zhang Z, Men Y (2012) Effect of annealing on the microstructure and mechanical properties of polypropylene with oriented shish-kebab structure. *Polym Int* 61(2):252–258
- Bai H, Wang Y, Zhang Z, Liang H, Li Y, Li L, Zhou Z, Men Y (2009) Influence of annealing on microstructure and mechanical properties of isotactic polypropylene with  $\beta$ -phase nucleating agent. *Macromolecules* 42(17):6647–6655
- Han L, Li X, Li Y, Huang T, Wang Y, Wu J, Xiang F (2010) Influence of annealing on microstructure and physical properties

- of isotactic polypropylene/calcium carbonate composites with  $\beta$ -phase nucleating agent. *Mater Sci Eng A* 527(13):3176–3185
9. Wang L, Zhang QP, Wang JH, Yang B, Yang MB, Feng JM (2014) Effects of annealing on the hierarchical crystalline structures and mechanical properties of injection-molded bars of high-density polyethylene. *Polym Int* 63(2):296–306
  10. Liu D, Jian K, Ming X, Cao Y (2013) Effect of annealing on phase structure and mechanical behaviors of polypropylene hard elastic films. *J Polym Res* 20(5):126
  11. Xu R, Sheng Z, Wang J, Jian K, Ming X, Feng Y (2018) Impact of different die draw ratio on crystalline and oriented properties of polypropylene cast films and annealed films. *J Polym Res* 25(6): 142
  12. Hedesiu C, §; Demco DE., ‡; Kleppinger R; Vanden Poel G; Gijsbers W; Blümich B; Remerie K, a.; VM (2007) Litvinov, effect of temperature and annealing on the phase composition, molecular mobility, and the thickness of domains in isotactic polypropylene studied by proton solid-state NMR, SAXS, and DSC. *Macromolecules* 40 (40), 3977–3989
  13. Yao YF, Graf R, Spiess HW, Rastogi S (2008) Restricted segmental mobility can facilitate medium-range chain diffusion: a NMR study of morphological influence on chain dynamics of polyethylene. *Macromolecules* 41(7):2514–2519
  14. Somani RH, Yang L, Zhu L, Hsiao BS (2005) Flow-induced shish-kebab precursor structures in entangled polymer melts. *Polymer* 46(20):8587–8623
  15. Zhang, A.; Xiao, C.; Wu, Y.; Li, C.; Ji, Y.; Li, L.; Hu, W.; Wang, Z.; Ma, W.; Li, W. (2016) Effect of Fluorination on Molecular Orientation of Conjugated Polymers in High Performance Field-Effect Transistors. *Macromolecules* 49 (17)
  16. Jiang J, Liu X, Lian M, Pan Y, Chen Q, Liu H, Zheng G, Guo Z, Schubert DW, Shen C (2018) Self-reinforcing and toughening isotactic polypropylene via melt sequential injection molding. *Polym Test* 67:183–189
  17. Mi D-S, Hou F-Y, Zhou M, Zhang J (2018) Distribution of  $\alpha$ -,  $\beta$ -, and  $\gamma$ -phases in a multi-flow injection-molded hierarchical structure. *Chin J Polym Sci* 6:1–11
  18. Wang X, Pan Y, Qin Y, Voigt M, Liu X, Zheng G, Chen Q, Schubert DW, Liu C, Shen C (2018) Creep and recovery behavior of injection-molded isotactic polypropylene with controllable skin-core structure. *Polym Test* 69:478–484
  19. Li Z, Bing N, Tian N, Lv R, Zou S (2011) Enhanced molecular orientation and strain hardening in melt-spun isotactic polypropylene monofilaments through partial melting recrystallization. *J Appl Polym Sci* 123(2):995–999
  20. Gross B, Peterman J (1984) Synergisms of mechanical properties in blends of semi-crystalline polymers. *J Mater Sci* 19(1):105–112
  21. Lotz B; Wittmann JC (2010) Polyethylene–isotactic polypropylene epitaxy: Analysis of the diffraction patterns of oriented biphasic blends. *J Polym Sci B Polym Phys* 25 (5), –
  22. Petermann J, Xu Y (1991) The origin of heteroepitaxy in the system of uniaxially oriented isotactic polypropylene and polyethylene. *J Mater Sci* 26(5):1211–1215
  23. Petermann J, Broza G, Rieck U, Kawaguchi A (1987) Epitaxial interfaces in semi-crystalline polymers and their applications. *J Mater Sci* 22(4):1477–1481
  24. Zhou M, Mi D, Hou F, Zhang J (2017) Tailored crystalline structure and mechanical properties of isotactic polypropylene/high molecular weight polyethylene blend. *Ind Eng Chem Res* 56(29):8385–8392
  25. Na B, Zhang Q, Wang K, Li L, Fu Q (2005) Origin of various lamellar orientations in high-density polyethylene/isotactic polypropylene blends achieved via dynamic packing injection molding: bulk crystallization vs. epitaxy. *Polymer* 46(3):819–825
  26. Su R, Wang K, Zhang Q, Chen F, Fu Q, Hu N, Chen E (2011) Epitaxial crystallization and oriented structure of linear low-density polyethylene/isotactic polypropylene blends obtained via dynamic packing injection molding. *Polym Adv Technol* 22(2): 225–231
  27. Su R, Wang K, Zhang Q, Chen F, Fu Q, Xu W, Na B (2009) Orientation and epitaxy in the injection-molded bars of linear low-density polyethylene/isotactic polypropylene blends: an infrared dichroism measurement. *J Phys Chem B* 113(21):7423–7429
  28. Zhi-hao; Zhao; Fei-fei; Wang; Zhou; Kai-zhi; Shen; Zhang (2016) Altering the Hierarchical Morphology Distribution of Injection Molded Polyethylene by the Introduction of Crosslink Network and Periodical Shear. *Chin J Polym Sci* 34 (12), 1479–1489
  29. Ren-xi; Qi-xiong; Zhou; Chao; Da-shan; Zhang (2015) The Banded Spherulites of iPP Induced by Pressure Vibration Injection Molding. *Chin J Polym Sci* 33 (11), 1625–1632
  30. Deng P, Whiteside B, Wang F, Norris K, Zhang J (2014) Epitaxial growth and morphological characteristics of isotactic polypropylene/polyethylene blends: scale effect and mold temperature. *Polym Test* 34:192–201
  31. Olley RH, Bassett DC (1982) An improved permanganic etchant for polyolefines. *Polymer* 23(12):1707–1710
  32. Shouke Yan DY (1998) Jürgen Petermann, controlling factors for the occurrence of heteroepitaxy of polyethylene on highly oriented isotactic polypropylene. *Polymer* 39(19):4569–4578
  33. Gu X, Wang Y, Jiang Y, Liu M, Fu Q, Zhang J (2019) High impact performance induced by a synergistic effect of heteroepitaxy and oriented layer-unoriented layer alternated structure in iPP/HDPE injection molded part. *Polymer* 175:206–214
  34. Niu B, Chen JB, Chen J, Xu J, Zhong GJ, Li ZM (2015) Crystallization of linear low density polyethylene on in situ oriented isotactic polypropylene substrate manipulated by extensional flow field. *Crystengcomm* 18(1):77–91
  35. Donnay M, Ponçot M, Tinnes JP, Schenk T, Ferry O, Royaud I (2017) In situ study of the tensile deformation micro-mechanisms of semi-crystalline POLY(ETHYLENE terephthalate) films using synchrotron radiation X-ray scattering. *Polymer* 117:268–281
  36. Housmans JW, Gahleitner M, Peters GWM, Han EHM (2009) Structure–property relations in molded, nucleated isotactic polypropylene. *Polymer* 50(10):2304–2319
  37. Liu X, Dai K, Hao X, Zheng G, Liu C, Schubert DW, Shen C (2013) Crystalline structure of injection molded  $\beta$ -isotactic polypropylene: analysis of the oriented shear zone. *Ind Eng Chem Res* 52(34):11996–12002

**Publisher's note** Springer Nature remains neutral with regard to jurisdictional claims in published maps and institutional affiliations.